NRC Research Press

NOTE

Field monitoring of the ground vibrations adjacent to an onshore wind turbine foundation

Pengpeng He, Jesús González-Hurtado, Tim Newson, Hanping Hong, Melanie Postman, and Sheri Molnar

Abstract: Investigations of the soil–foundation interaction behaviour of wind turbine foundations and transfer of energy from the wind to the ground have not been reported in Canada. Indeed, very few vibration monitoring studies have been conducted globally around wind farms. It has been found that turbines predominantly produce vibrations related to structural resonances and blade-passing frequencies. Energy is found to be modified with distance and is dominated by surface waves. This paper describes a study of the effect of wind–structure interaction on the behaviour of a turbine foundation and the generation of ground-based vibrations around a working commercial wind turbine in Ontario. The field monitoring system and meteorological instrumentation are described in this paper and the responses of the structure and surrounding ground due to the fluctuating wind-field are discussed. The spectral analysis shows that the higher frequency vibrations attenuate more rapidly than the lower frequency vibrations. The tilted elliptical particle motions are found to be non-Gaussian because of the non-Gaussian wind conditions. The response attenuation with distance indicates that both geometric and material attenuation may dominate the vibration attenuation in the near field and only geometric attenuation occurs in the far field.

Key words: wind turbine, foundation vibration, ground vibration, wind, soil–foundation interaction.

Résumé : Des enquêtes sur le comportement des fondations d'éoliennes en matière d'interaction sol–fondation et de transfert d'énergie du vent au sol n'ont pas été signalées au Canada. En effet, très peu d'études de surveillance des vibrations ont été menées à l'échelle mondiale autour des parcs éoliens. Il a été constaté que les turbines produisent principalement des vibrations liées aux résonances structurelles et aux fréquences de passage des pales. On constate que l'énergie se modifie avec la distance et qu'elle est dominée par les ondes de surface. Cet article décrit une étude de l'effet de l'interaction entre le vent et la structure sur le comportement des fondations d'une turbine et la production de vibrations au sol autour d'une turbine éolienne commerciale en fonctionnement en Ontario. Le système de surveillance sur le terrain et l'instrumentation météorologique sont décrits dans ce document et les réactions de la structure et du sol environnant dues à la fluctuation du champ de vent sont examinées. L'analyse spectrale montre que les vibrations de haute fréquence s'atténuent plus rapidement que les vibrations de basse fréquence. Les mouvements elliptiques inclinés des particules s'avèrent être non gaussiens en raison des conditions de vent non gaussiennes. L'atténuation de la réponse avec la distance indique que l'atténuation géométrique et matérielle peut dominer l'atténuation des vibrations dans le champ proche et que seule l'atténuation géométrique se produit dans le champ lointain. [Traduit par la Redaction]

Mots-clés : turbine éolienne, vibration des fondations, vibration du sol, vent, interaction sol–fondation.

Introduction

Wind is a major source of renewable energy and has been the largest source of new electricity in Canada for the last 11 years. Wind turbines are subjected to millions of load cycles throughout their service lives due to environmental and mechanical loads. Understanding the response of wind turbine foundations to this complex cyclical vertical–horizontal–moment loading plays an important role in turbine design. Investigations of the soil–foundation interaction behaviour and transfer of energy from the wind through an onshore turbine tower to the ground and the subsequent transmission of elastic waves to the surrounding areas have not been reported in Canada. Indeed, very few vibration monitoring studies have been conducted globally around onshore wind farms. Saccorotti et al. (2011) and Xi Engineering Consultants Ltd. (2014) found that turbines predominantly produce vibrations related to structural resonances and blade-passing frequencies. Spectral peaks correlated with wind speed and spectral composition, and energy was significantly modified with distance and was dominated by surface waves. Further studies by Styles et al. (2005) and Fiori et al. (2009) found maximum root mean square (RMS) velocities on turbine foundations ranging between 0.07 and 0.15 mm/s. Edwards (2015) found RMS velocities of 0.001 mm/s at 125 m from a specific turbine.

The prediction of vibration propagation through the ground can be rather difficult due to the complexities involved in field soil properties, modelling of vibration sources, and resulting

Received 17 December 2019. Accepted 2 May 2020.

P. He, J. González-Hurtado,* and T. Newson. Geotechnical Research Centre, Department of Civil Engineering, Western University, London, ON N6A 5B9, Canada.
H. Hong. Department of Civil Engineering, Western University, London, ON N6A 5B9, Canada.
M. Postman and S. Molnar. Department of Earth Sciences, Western University, London, ON N6A 5B7, Canada.
Corresponding author: Tim Newson (email: tnewson@eng.uwo.ca).
*Present address: Golder Associates Ltd., 309 Exeter Road, London, ON N6L 1C1, Canada.

J_ID: CGJ ART NO: cgj-2019-0828 Date: 20-March-21 Page: 596 Total Pages: 8 4/Color Figure(s): "F1, F3-F6"

near- and far-field behaviour (Richart et al. 1970). Generally, the ground vibration amplitude attenuates with distance due to geometric and material damping (Woods and Jedele 1985). As demonstrated by some researchers (e.g., Gutowski and Dym 1976; Taniguchi and Sawada 1979; Kim and Lee 2000), the propagation and attenuation characteristics of vibrations highly depend on the type of vibration source and the geotechnical properties of a site. In Ontario, a minimum offset distance of 550 m between residents and vibration sources, such as wind turbines, is mandatory. However, this distance seems to be related to acoustic criteria and is less than the minimum offset distance mandated by most other jurisdictions in North America and Europe. Further work is needed to help establish the distances at which the elastic wavefields at the base of the wind turbine structures is no longer present (or sensible) with distance, to better understand the significance of setback distances.

A multi-disciplinary research project is underway to investigate the behaviour of a commercial wind turbine founded on a shallow foundation in Southern Ontario. One goal of the project is to provide understanding of the effect of the wind–structure interaction on the behaviour of the turbine foundation and the generation of ground-based vibrations around the turbine. A detailed site investigation has been conducted previously on the site and a full-scale monitoring system has been installed on the wind turbine. The field foundation monitoring system and meteorological instrumentation are described in this paper and typical responses of the foundation and the surrounding ground due to the structural response of the turbine during monitoring are discussed.

Site conditions

The wind turbine in this study is located in the Great Lakes region of Southern Ontario (due to commercial sensitivities the exact site location cannot be disclosed). This specific turbine model produces a nominal power of 2.3 MW, has a hub height of 80 m, and triple blade rotor with a 93 m diameter. The wind turbine is supported by a shallow octagonal foundation, with approximate dimensions of 19 m in diameter and 3 m in thickness. A meteorological tower featuring five anemometers at different heights (from 35 to 80 m above ground level) is located 150 m northwest of the wind turbine.

Soil profile from field and laboratory data

To characterize the soil profile at the site, four boreholes were drilled adjacent to the turbine foundation to depths twice the foundation diameter. Soil samples were collected at 3 m depth intervals. In situ testing was also performed and consisted of seismic cone penetration testing (SCPTu) and cross-hole seismic testing (CST). To complement the in situ testing, various laboratory tests were carried out as well including consolidated isotropic undrained triaxial (CIU) tests, oedometer tests, bender element (BE) tests, and resonant column (RCA) tests. For more detailed information on the testing results refer to previous papers and reports from the authors (González-Hurtado and Newson 2014, 2016; Tyldesley et al. 2013; Kiss 2014, 2016).

The deposit can be approximately split into three different layers: a heavily weathered oxidized upper crust between 0 and 1.5 m, a partially weathered lower crust that transitions from an oxidized to an unoxidized state between 1.5 and 4.5 m, and an unweathered clay till from 4.5 to 40 m. Figure 1 shows the shear wave velocity (V_s) profiles derived from in situ cross-hole, SCPTu, RCA, and BE testing. It shows that V_s reduces rapidly to relatively uniform values at depths of 6 to 8 m, maintaining this trend in the underlying 12 to 15 m. The wind turbine foundation sits in the partially weathered lower crust, with a foundation embedment depth of 3 m.

Fig. 1. Shear wave velocity with depth. [Colour online.]

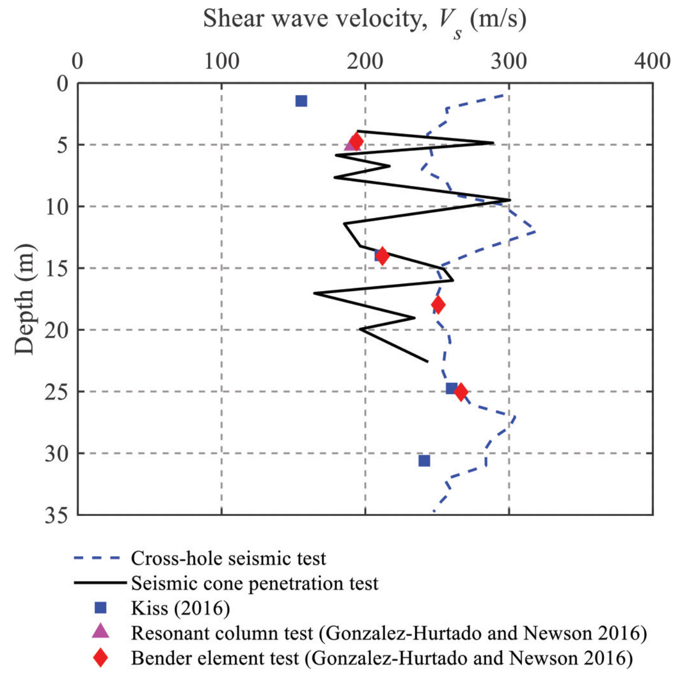

IEC classification and design wind speeds

IEC 61400-1 (IEC 2019) is a commonly used design standard in North America and Europe for wind turbines of all sizes. This wind farm has been classified as a Class IIb site using IEC 61400-1, with the expected turbulence intensity equal to 14% at 15 m/s. The reference wind speed average over 10 min with a 50 year return period at hub height (80 m) is specified as 42 5 m/s and the corresponding site-specific value has been estimated to be 33.9 m/s (this value is provided by the design report based on site meteorological data and a study by the authors (González-Hurtado 2019)).

Field monitoring system

Foundation and wind monitoring

The current foundation monitoring system includes four uniaxial tiltmeters (recording angles of inclination), three portable high-frequency triaxial seismometers (known as Tromino; recording velocities of vibrations), and one triaxial accelerometer (recording accelerations of vibrations), as shown in Fig. 2. The sampling rates of the tiltmeter, Trominos, and accelerometer are 20, 128, and 20 Hz, respectively. Results from the tiltmeters (denoted as TM1, 2, 3, and 4 in Fig. 2) have been reported previously by Kiss et al. (2014) and will not be repeated here. The accelerometer is installed at the same position as TM2, and the Trominos are located at 30 (N1), 130 (N2), and 300 m (N3) to the north of the foundation edge. The 30 m N1 was chosen as the closest Tromino location to the wind turbine, as 30 m represents one-third of the blade diameter and was far enough not to be influenced by the top of the 19 m diameter foundation and the turbine substation. The distances of N2 and N3 are more appropriate to accommodate the exponential decrease of vibrations with distance and the maximum distance of 300 m was chosen due to the potential interference from neighbouring turbines. Vibrations towards the N and E cardinal directions have been taken as positive. In this paper, only data obtained from N0 to N3 are used to analyze the wave propagation induced by the vibration of the wind turbine foundation.

Fig. 2. Diagram of foundation and location of the instrumentation (all dimensions in metres; not to scale).

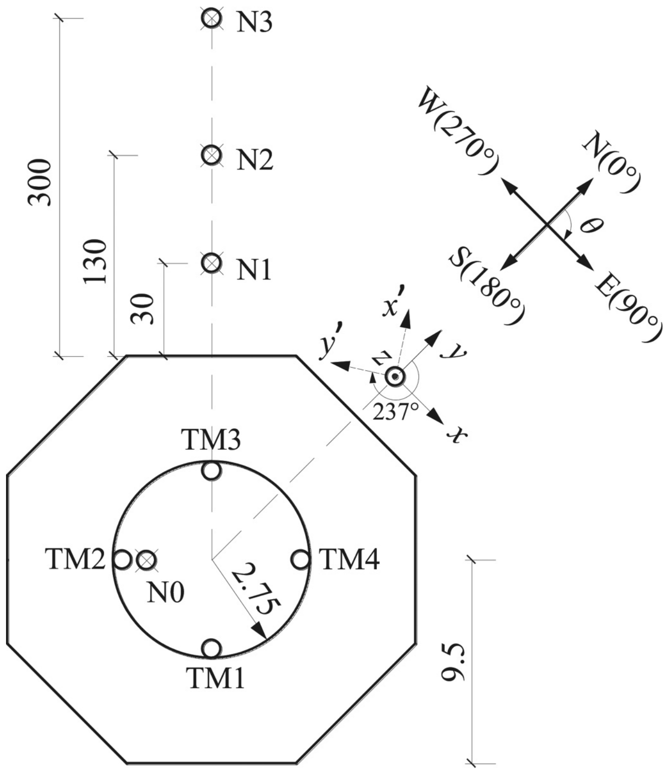

Wind speed and direction variation over the study time period was characterized to relate the response of the foundation to the incoming wind field. In this paper, only the wind data (speed and direction) measured at the hub height (80 m) is reported. This anemometer sampled at 1 Hz.

Recorded data

Typical foundation data and analysis

Table 1 shows the recording periods of the triaxial accelerometer (N0, located on the foundation edge) and the Trominos (N1 to N3). The recording period of the wind was over 2 days in October 2016, but only the period corresponding to that of the Trominos was extracted.

The measured wind speed and direction (measured clockwise from the north) over the study period are shown in Fig. 3. As shown in Fig. 3*a*, the wind speed remains relatively stable except for a slight increase during the last 2000 s. The mean and RMS values of the wind speed are 9.85 and 1.31 m/s, respectively. Following the definition of turbulence intensity (Burton et al. 2001), the turbulence intensity of the wind is 0.13. The wind direction was primarily from the southwest to west–southwest direction (220°~250°). Overall, the wind speed and direction did not change significantly, allowing a reasonable characterization of the statistics of the behaviour of the wind and soil vibrations.

Figure 4 illustrates the time-history and power spectral density of the acceleration in the positive *x* (eastern) direction at N0 and N3. It is obvious that the acceleration amplitude at N0 on the foundation is much higher than that at N3 due to the proximity of the vibration source. Figure 4*a* shows that the positive part of the acceleration is higher and fluctuates more than the negative part of the acceleration. This may be attributed to two reasons: firstly, the turbine wake flow can induce a negative pressure at the back of the wind turbine, pulling the wind turbine in the positive *x* direction; secondly, the wind direction is in the southwest direction, which is not consistent with the positive *x* direction of the accelerometer at N0 (see Fig. 2). The corresponding power spectral density (PSD) is shown in Figs. 4*c* and 4*d*. PSD is used to describe the spectral energy distribution with frequencies so that the dominant frequency ranges can be specified. As shown in Fig. 4*c*, the frequency measured at N0 is widely distributed in the range from 0 to 8 Hz. The PSD at N0 peaks at around 0.2–0.5 Hz and gradually decreases to zero with frequency. Interestingly, the PSD at N3 (see Fig. 4*d*) has a peak corresponding to a higher frequency, ranging from 40 to 55 Hz, probably because of wave dispersion in the soil.

Table 1. Recording times of N1, N2, N3, and wind speed.

Sensor location	Time recorded
N0 (0 m)	1 h 19′ 14″
N1 (30 m)	1 h 28′ 37″
N2 (130 m)	1 h 40′ 47″
N3 (300 m)	0 h 42′ 31″
Wind	1 h 40′ 47″

To better distinguish the characteristics of the waves propagating through the soil, the particle motion data at N1 were subdivided into 10 and 1 min data blocks, as shown in Fig. 5. To analyze the effect of wind directions, the measured data in the *x* and *y* directions for each data block were transformed to the along-wind (x') and cross-wind (y') directions based on the mean wind direction of the corresponding block. As shown in Fig. 5, the along-wind vs. vertical direction motions are approximately counterclockwise ellipses and the cross-wind vibration is smaller compared with the vertical and along-wind vibration. Previous investigations of the along-wind and cross-wind responses of tall buildings (e.g., Melbourne 1975) have generally shown weak correlations, suggesting independence of the motions and excitation mechanisms. The response of most structures in the along-wind direction originates from the action of the incident turbulence of the longitudinal component of the wind velocity. In contrast, the cross-wind response is more complex and associated with the wake, incident turbulence, and cross-wind displacements. Motions from physical models and field monitoring of tall buildings have found joint probability distributions similar to bivariate Gaussian distributions.

Therefore, the particle motions in two directions for each data block (10 and 1 min) were considered to be two random variables of a bivariate Gaussian distribution with model parameters estimated using the Maximum Likelihood Estimation (MLE), i.e., maximizing the likelihood function to obtain the distribution parameters (Little and Rubin 2019). The Chi-Square Goodness of the fitting of the 1 min blocks shows that only 31.8% of the blocks in the $x'-z$ direction, 11.4% in the $y'-z$ direction, and 9.1% in the $x'-y'$ direction can be simulated with the bivariate Gaussian distribution (P-value > 0.05), while none of the 10 min blocks has a good fit. One 1 min block with a good fit is shown in Figs. 5*d*–5*f*, and the statistical parameters for the whole data are listed in Table 2. The contour plots obtained from the fitted bivariate Gaussian distribution represent the joint probability density, i.e., each ellipse means the joint probability density with a constant value. Many researchers studying wind loads on turbines from atmospheric turbulence assume that the turbulence inflow velocity field is Gaussian (Berg et al. 2016) and a number of models used by IEC 61400-1 (IEC 2019) and other design standards have been developed on this basis. However, it is known that turbulent atmospheric conditions can be non-Gaussian (particularly at smaller scales) for complex terrain and convective boundary

Fig. 3. Measured (*a*) wind speed and (*b*) wind direction. [Colour online.]

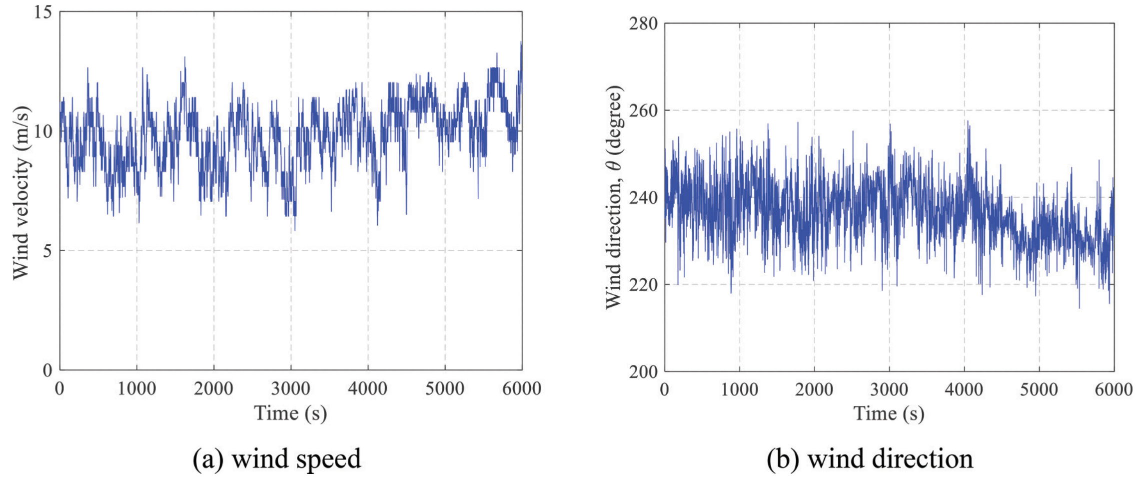

Fig. 4. Time-history and power spectral density of the acceleration in the *x* direction at locations N0 and N3: (*a*) time-history N0; (*b*) time-history N3; (*c*) power spectral density N0; and (*d*) power spectral density N3. [Colour online.]

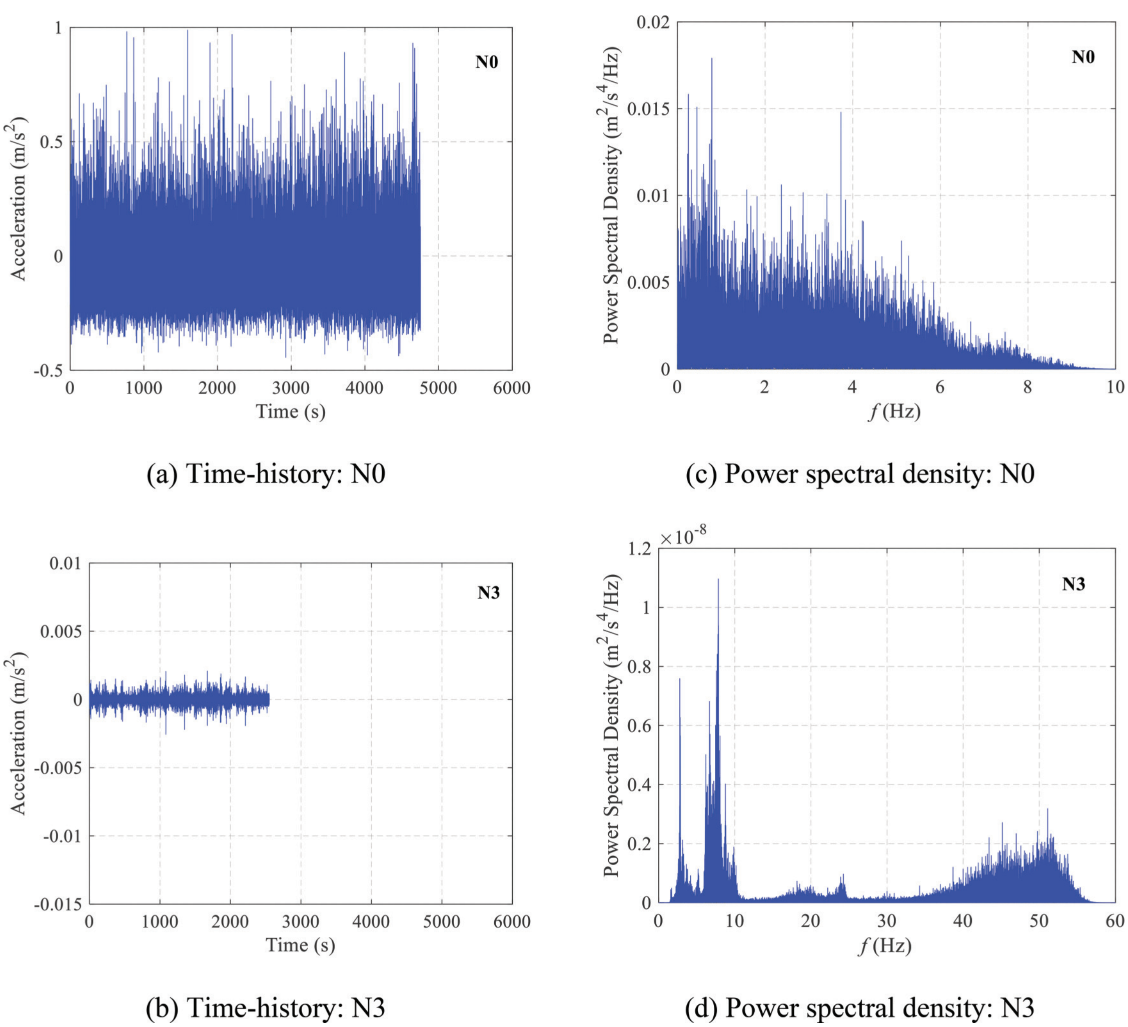

J_ID: CGJ ART NO: cgj-2019-0828 Date: 20-March-21 Page: 599 Total Pages: 8 4/Color Figure(s): "F1, F3-F6"

Fig. 5. One 10 min block of the measured particle motions and one 1 min block of the measured particle motions with fitted bivariate normal distribution at N1: (*a*) 10 min block, along-wind vs. vertical; (*b*) 10 min block, cross-wind vs. vertical; (*c*) 10 min block, along-wind vs. cross-wind; (*d*) 1 min block, along-wind vs. vertical; (*e*) 1 min block, cross-wind vs. vertical; and (*f*) 1 min block, along-wind vs. cross-wind. [Colour online.]

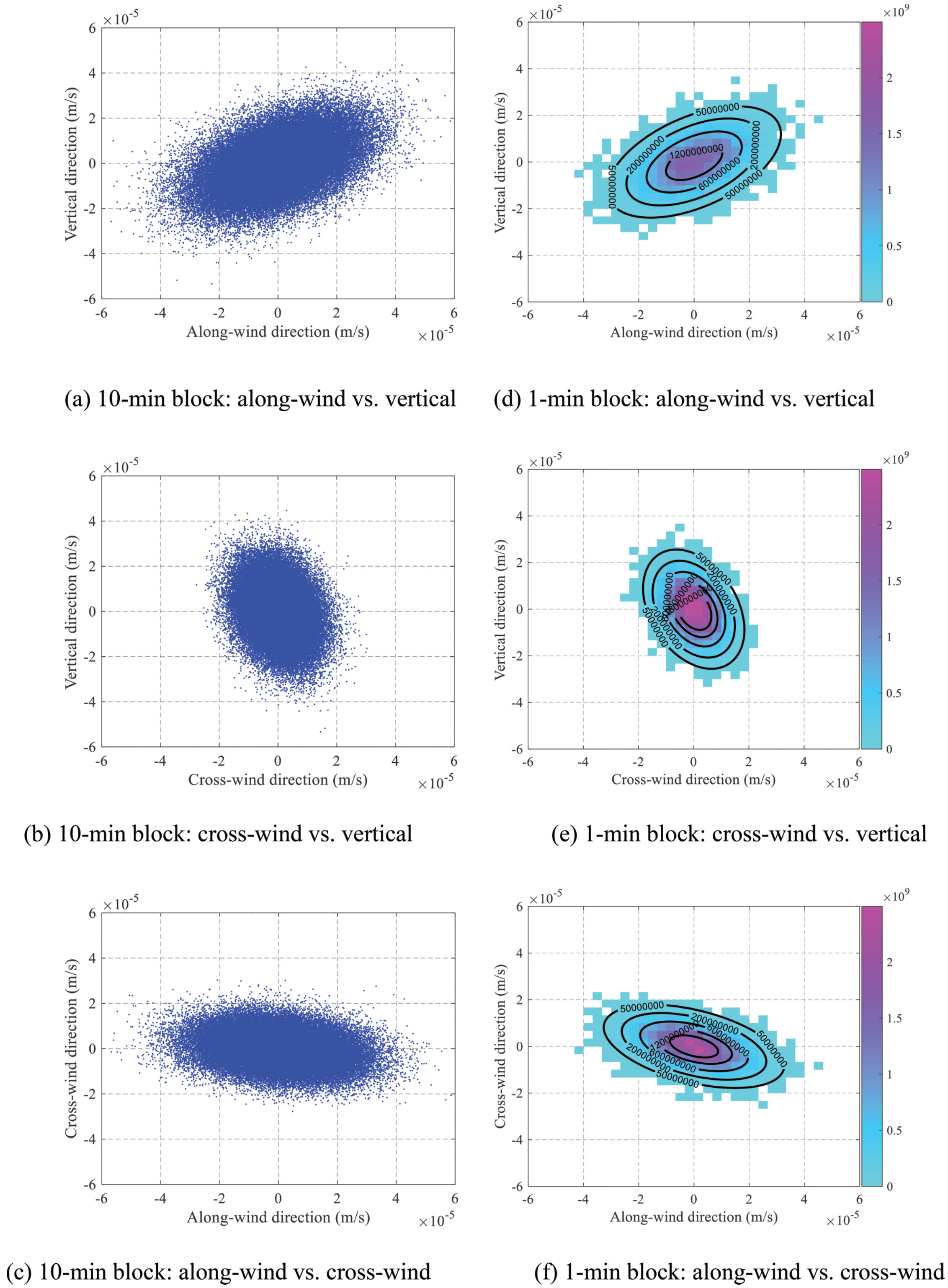

Table 2. Statistical parameters.

Location, direction	N1, $x'-z$	N1, $y'-z$	N1, $x'-y'$
Mean, μ (m/s)	-2.94×10^{-10} (x') -1.07×10^{-10} (z)	-0.80×10^{-10} (y') -1.07×10^{-10} (z)	-2.94×10^{-10} (x') -0.80×10^{-10} (y')
Standard deviation, σ (m/s)	1.27×10^{-5} (x') 1.01×10^{-5} (z)	0.66×10^{-5} (y') 1.01×10^{-5} (z)	1.27×10^{-5} (x') 0.66×10^{-5} (y')
Correlation coefficient, ρ	0.4741	−0.3051	−0.2928

Fig. 6. Velocity attenuation with distance: (*a*) along-wind direction and (*b*) cross-wind direction. [Colour online.]

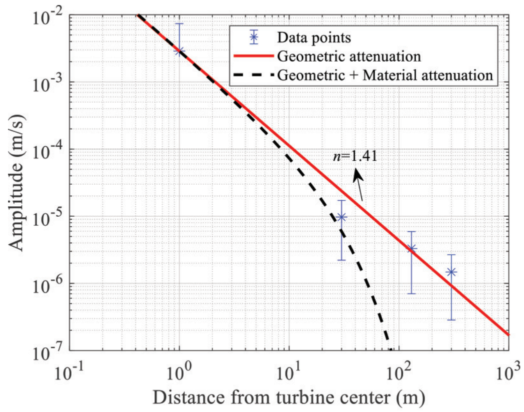

(a) Along-wind direction

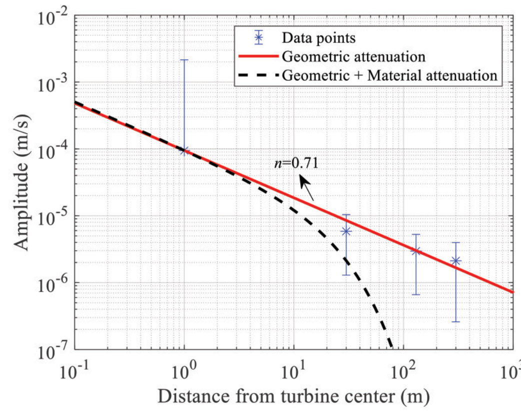

(b) Cross-wind direction

layers. McWilliams et al. (1979) showed that the longitudinal and transverse components of the wind velocity can be reasonably fitted with a bivariate Gaussian distribution. However, due to the varying longitudinal direction of the wind speed (more evident for larger time scales), the decomposed responses in the averaged x' and y' directions are unlikely to follow the same distribution as the wind velocity. For shorter time scales (e.g., 1 min blocks), the variations of the wind direction tend to be reduced and the fit of the bivariate Gaussian distribution seems to be improved (suggesting improved stationarity). Non-Gaussian multi-variate approaches may provide better fits to the data with more appropriate skewness and kurtosis. This may have implications with respect to fatigue analysis and estimates of component life spans, as higher peakness and heavier tails of the distributions will change the expected loading history of the turbines.

For the successful bivariate fits, Table 2 shows that the mean values of the velocities are essentially zero. The correlation coefficients of the motions show that the $x'-z$ (correlation coefficient, ρ = 0.4741) direction motions at N1 are more highly correlated than those in the $y'-z$ (ρ = −0.3051) and $x'-y'$ (ρ = −0.2928) directions. These along-wind and cross-wind responses have weak dependence upon each other, which coincides with the typical conclusion for symmetrical tall buildings (Melbourne 1975).

Although ground wave types and characteristics from operating wind turbines are not well understood, Westwood and Styles (2017) identified a range of both surface and body waves propagating from wind turbines. They determined that the turbines were a constant source of multiple types of waves arriving simultaneously and out of phase (i.e., Rayleigh and Love, and SH and SV). A consequence of material dispersion on the propagation of Rayleigh waves in viscoelastic media is that the principal axes of the particle orbits are sloping. The degree of rotation depends on the material properties (Borcherdt 1973; Bath and Berkhout 1986; Kim and Lee 2000). This can be observed in the plots of vertical and along-wind displacements. However, there are also significant cross-wind direction displacements evident, suggesting simultaneous Love waves occurring. Crampin (1975) and Tanimoto (2004) also noted that these types of tilted elliptical particle motions occur with surface waves propagating through anisotropic and layered media and the tilt angle of the ellipse is associated with the orientation of the anisotropy with respect to the direction of propagation. This deposit has been characterized as having horizontal stiffness higher than the vertical stiffness (González-Hurtado and Newson 2016). In this type of material, the particle motions remain elliptical, but the plane of polarization deviates from the propagating direction by a certain angle, leading to a more complex three-dimensional quasi-Rayleigh behaviour with additional transverse soil motions.

Due to the low dominant frequencies (0.2~0.5 Hz) at N0, the dynamic soil–foundation interaction can be relatively small (Tileylioglu et al. 2011) and the vibrations at N0 can thus be considered to be an approximation of the vibrations of the ground beneath the foundation. The velocity attenuation in the soil with distance along the ground surface is illustrated in Fig. 6. The mean values and standard deviation of the velocities are represented by the error bars. The figure shows that the along-wind and cross-wind attenuation is similar. The attenuation relationship is evaluated with the following equation (Kim and Lee 2000):

$$w_2 = w_1 \left(\frac{r_1}{r_2}\right)^n e^{-\alpha(r_2 - r_1)} \tag{1}$$

where w_2 and w_1 are the amplitudes at distances r_2 and r_1 from the vibration source, respectively; n and α are geometric and material damping coefficients, respectively. α can be evaluated using

$$\alpha = \frac{\pi \eta f}{c} \tag{2}$$

where η is a loss factor related to the hysteretic damping of the ground; f is the wave frequency; c is the wave propagation velocity. As described above, the propagating wave has been assumed to be primarily a Rayleigh wave, so Rayleigh wave velocity is used in eq. 2. The average Rayleigh wave velocity of the ground soil is estimated to be 262.8 m/s from the cross-hole testing. According to Fig. 4, the dominant frequency of 8 Hz was selected. The value of η is given as 0.5 for clay by Gutowski and Dym (1976). Therefore, α can be calculated as 0.0478 for both along-wind and cross-wind directions.

To examine the effect of the geometric and material damping, two fitting curves are applied: one considers only the geometric attenuation using $\alpha = 0$, the other one accounts for both the geometric and material attenuation using $\alpha = 0.0478$. As shown in Fig. 6, the fitted geometric damping coefficients in the along-wind and cross-wind directions are 1.41 and 0.71, respectively, without considering material attenuation. In contrast, the presence of material attenuation significantly increases the attenuation rate with distance. Comparison shows that primarily geometric attenuation can favorably describe the observed attenuation of the vibration amplitudes.

The value of n is related to the source type and the form of wave propagation. Gutowski and Dym (1976) reported values of n from different vibration field cases, e.g., traffic and train lines, pile driving, hydraulic compaction, and blasting. These values ranged from 0 to 2 depending on the nature of the waves (surface or body) and type of source (surface or buried and line or point). A point source producing purely Rayleigh waves in a homogeneous isotropic elastic half-space would have a value of $n = 1.5$, which is close to that found in the along-wind direction.

Summary and conclusions

The dynamic response of a wind turbine, located in the Great Lakes region of Southern Ontario, has been investigated with field tests. The wind data, shallow foundation vibration data, and ground motion data were obtained and analyzed.

The comparison between the dominant frequency ranges at different locations shows that higher frequency vibrations attenuate more rapidly than lower frequency vibrations. The observed propagating elastic wave front at some distance from the turbine appears to be dominated by surface waves and shows some influence of the presence of anisotropy or layering in the soil profile.

The vibration of the foundation appears to decrease rapidly with distance from the foundation. The analysis indicates that the geometric attenuation plays a more important role than the material attenuation for this site. The comparison between the two fitting curves in Fig. 6 shows that the discrepancy increases with distance and the recorded data coincide with the geometric attenuation, which indicates that the effect of material damping is negligible in the far field for this site. From the analysis of Kim and Lee (2000), the combination of these two attenuation factors can favorably describe the amplitude attenuation relationship with distance in the near field (within 100 m). Therefore, the vibration attenuation may be dominated by both geometric and material attenuation in the near field, whilst only geometric attenuation occurs in the far field.

The "subset" of the data presented in this paper is consistent with a full recorded dataset, which examined vibrations in two other directions (west and south) from the turbine. No dependence of recording location and wind direction was found (Postman 2017). Further work is required to confirm these findings for a larger range of wind speeds and directions, and different locations around the site, as well as for different operating conditions of the turbine.

Acknowledgements

The authors would like to acknowledge the help of J.J. Davis from Kruger Energy and the Western CES Seed Grant fund. The financial support of NSERC for the first and second authors is acknowledged. The first author is also grateful for the financial support of China Scholarship Council (CSC).

References

Bath, M., and Berkhout, A.J. 1986. Mathematical aspects of seismology: Handbook of geophysical exploration. Geophysical Press, London, UK.

Berg, J., Natarajan, A., Mann, J., and Patton, E.G. 2016. Gaussian vs non-Gaussian turbulence: impact on wind turbine loads. Wind Energy, **19**(11): 1975–1989. doi:10.1002/we.1963.

Borcherdt, R.D. 1973. Rayleigh-type surface wave on a linear viscoelastic half-space. The Journal of the Acoustical Society of America, **54**(6): 1651–1653. doi:10.1121/1.1914463.

Burton, T., Sharpe, D., Jenkins, N., and Bossanyi, E. 2001. Wind energy handbook. John Wiley & Sons, Inc, Hoboken, N.J.

Crampin, S. 1975. Distinctive particle motion of surface waves as a diagnostic of anisotropic layering. Geophysical Journal International, **40**(2): 177–186. doi:10.1111/j.1365-246X.1975.tb07045.x.

Edwards, W. N. 2015. Analysis of measured wind turbine seismic noise generated from the Summerside Wind Farm, Prince Edward Island. Open File 7763. Geological Survey of Canada, Natural Resources Canada, Ottawa, ON.

Fiori, I., Giordano, L., Hild, S., Losurdo, G., Marchetti, E., Mayer, G., and Paoletti, F. 2009. A study of the seismic disturbance produced by the wind park near the gravitational wave detector. *In* Proceedings of 3rd International Conferences on Wind Turbine Noise, Aalborg, Denmark, 17–19 June 2009. International Institute of Noise Control Engineering/Europe, Southport.

González-Hurtado, J. 2019. The effect of stiffness anisotropy of a glacial clay on the behaviour of a shallow wind turbine foundation. Ph.D. thesis, Department of Civil and Environmental Engineering, Western University, London, ON.

González-Hurtado, J., and Newson, T. 2014. Determination of rigidity index for a shallow foundation on a carbonate clay till. *In* Proceedings of the 67th Canadian Geotechnical Conference., Regina, SK, 28 September – 1 October 2014. Canadian Geotechnical Society, Vancouver, Paper # 227.

González-Hurtado, J., and Newson, T. 2016. Small-strain behaviour of a carbonate clay till underlying a wind turbine shallow foundation by different in-situ and laboratory tests. *In* Proceedings of the 69th Canadian Geotechnical Conference, Vancouver, B.C., 2–5 October 2016. Canadian Geotechnical Society, Vancouver. Paper No. 3653.

Gutowski, T.G., and Dym, C.L. 1976. Propagation of ground vibration: a review. Journal of Sound and Vibration, **49**(2): 179–193. doi:10.1016/0022-460X(76)90495-8.

IEC. 2019. Wind energy generation systems - Part 1: Design requirements. IEC 61400-1. International Electrotechnical Commission, Geneva, Switzerland.

Kim, D.S., and Lee, J.S. 2000. Propagation and attenuation characteristics of various ground vibrations. Soil Dynamics and Earthquake Engineering, **19**(2): 115–126. doi:10.1016/S0267-7261(00)00002-6.

Kiss, J. 2016. Evaluation of the response of carbonate clay beneath a wind turbine foundation. M.Sc. thesis, Department of Civil and Environmental Engineering, Western University, London, ON.

Kiss, J., Newson, T., Miller, C., and Carriveau, R. 2014. The effect of wind-structure interaction on the behavior of a shallow wind turbine foundation. *In* Proceedings of the 67th Canadian Geotechnical Conference., Regina, SK, 28 September – 1 October 2014. Canadian Geotechnical Society, Vancouver. Paper No. 231.

Little, R.J., and Rubin, D.B. 2019. Statistical analysis with missing data. Vol. 793. John Wiley & Sons, Hoboken, US.

McWilliams, B., Newmann, M.M., and Sprevak, D. 1979. The probability distribution of wind velocity and direction. Wind Engineering, **3**: 269–273.

Melbourne, W.H. 1975. Probability distributions of response of BHP house to wind action and model comparisons. Journal of Wind Engineering and Industrial Aerodynamics, **1**: 167–175. doi:10.1016/0167-6105(75)90012-4.

Postman, M. 2017. Vibration monitoring at a wind turbine site in Port Alma, Ontario. B.Sc. thesis, Department of Earth Sciences, Western University, London, ON.

Richart, F.E., Hall, J.R., and Woods, R.D. 1970. Vibrations of soils and foundations. Prentice-Hall.

Saccorotti, G., Piccinini, D., Cauchie, L., and Fiori, I. 2011. Seismic noise by wind farms: a case study from the Virgo Gravitational Wave Observatory. Bulletin of the Seismological Society of America, **101**(2): 568–578. doi:10.1785/0120100203.

Styles, P., Stimpson, I., Toon, S., England, R., and Wright, M. 2005. Microseismic and infrasound monitoring of low frequency noise and vibrations from windfarms: recommendations on the siting of windfarms in the vicinity of Eskdalemuir, Scotland. Report for the Ministry of Defence, 18. Keele University, Staffordshire, UK.

Taniguchi, E., and Sawada, K. 1979. Attenuation with distance of traffic-induced vibrations. Soils and Foundations, **19**(2): 15–28. doi:10.3208/sandf1972.19.2_15.

Tanimoto, T. 2004. The azimuthal dependence of surface wave polarization in a slightly anisotropic medium. Geophysical Journal International, **156**(1): 73–78. doi:10.1111/j.1365-246X.2004.02130.x.

Tileylioglu, S., Stewart, J.P., and Nigbor, R.L. 2011. Dynamic stiffness and damping of a shallow foundation from forced vibration of a field test structure. Journal of Geotechnical and Geoenvironmental Engineering, **137**(4): 344–353. doi:10.1061/(ASCE)GT.1943-5606.0000430.

Tyldesley, M., Newson, T., Boone, S., and Carriveau, R. 2013. Characterization of the geotechnical properties of a carbonate clayey silt till for a shallow wind turbine foundation. *In* Proceedings of the 18th International Conference on Soil Mechanics and Geotechnical Engineering, Paris, France, 2–6 September 2013. The French Society for Soil Mechanics and Geotechnical Engineering, Paris, pp. 2407–2410.

Westwood, R.F., and Styles, P. 2017. Assessing the seismic wavefield of a wind turbine using polarization analysis. Wind Energy, **20**(11): 1841–1850. doi:10.1002/we.2124.

Woods, R.D., and Jedele, L.P. 1985. Energy—attenuation relationships from construction vibrations. *In* Proceedings of Vibration problems in geotechnical engineering, Detroit, M.I., 22 October 1985. American Society of Civil Engineers, Reston, pp. 229–246.

Xi Engineering Consultants Ltd. 2014. Seismic vibration produced by wind turbines in the Eskdalemuir region. Report No. FMB_203_FINAL_V5R, Xi Engineering Consultants Ltd., Edinburgh, UK.